Analysis Tools for Next Generation Hadron Spectroscopy Experiments

February 13, 2014

Contents

Preface

The series of workshops on *New Partial-Wave Analysis Tools for Next Generation Hadron Spectroscopy Experiments* was initiated with the ATHOS12 meeting, which took place in Camogli, Italy, June 20–22, 2012. It was followed by ATHOS13 in Kloster Seeon near Munich, Germany, May 21–24, 2013. The ATHOS15 meeting is planned for 2015 in the USA.

The workshops focus on the development of amplitude analysis tools for meson and baryon spectroscopy, and complement other programs in hadron spectroscopy organized in the recent past including the INT-JLab Workshop on Hadron Spectroscopy in Seattle in 2009, the International Workshop on Amplitude Analysis in Hadron Spectroscopy at the ECT*-Trento in 2011, the School on Amplitude Analysis in Modern Physics in Bad Honnef in 2011, the Jefferson Lab Advanced Study Institute Summer School in 2012, and the School on Concepts of Modern Amplitude Analysis Techniques in Flecken-Zechlin near Berlin in September 2013.

The aim of this document is to summarize the discussions that took place at the ATHOS12 and ATHOS13 meetings. We do not attempt a comprehensive review of the field of amplitude analysis, but offer a collection of thoughts that we hope may lay the ground for such a document.

The Editorial Board

Marco Battaglieri
Bill Briscoe
Su-Urk Chung
Geoffrey Fox
Bernhard Ketzer
Vincent Mathieu
Adam Szczepaniak

1 Introduction

[C.Hanhart, M.Hoferichter, B.Kubis]

Quantum Chromodynamics (QCD), the fundamental theory of the strong interactions, defines the interactions of quarks and gluons, both types carrying the so-called color charge, that form the fundamental constituents of hadrons.[1] At high energies, these partons become asymptotically free, and systematic calculations based on perturbation theory in the strong coupling constant are possible and extremely successful. However, especially inside light hadrons that are in the focus of this manuscript, the average energies and momenta of partons are below the scale at which perturbation theory can be justified, and hadron properties are determined by interactions that are genuinely non-perturbative in nature. In particular, the bulk of hadron masses originates from gluonic self-interactions, which lead to forces that bind the constituents within distances smaller than 10^{-15} m in a way that only allows objects neutral with respect to the color charge to exist as physical, asymptotic states—a phenomenon known as confinement. As a consequence, the elementary degrees of freedom of the underlying theory only manifest themselves indirectly in the physical spectrum, which instead is built from composite, colorless hadrons. Just as atomic spectroscopy was instrumental in elucidating the underlying electromagnetic interactions, hadron spectroscopy is therefore the foremost laboratory for studying the implications of QCD.

While for many years the quark model has provided the main template for the spectrum of hadrons, recent developments in lattice simulations on the one side and effective-field-theory methods on the other have opened new avenues for investigations of hadron properties that are rooted in QCD. One of the most mysterious parts of the spectrum concerns the phenomenology of low-energy gluons and thus a complete mapping of gluonic excitations—that may manifest themselves either in hybrid states (states with both quarks and gluons a active, valence degrees of freedom) or in glue balls (states formed from gluons only)—is a central part of the present and future investigation of the hadron spectrum.

The anticipated accuracy of the next-generation hadron spectroscopy experiments will in principle allow for the identification of hadronic resonances for which either a reliable determination of their resonance parameters has proven elusive or even their very existence could not be unambiguously established before. Frequently, their identification is complicated by the occurrence of overlapping resonances, pole positions far in the complex plane, or weak couplings to the channels experimentally accessible. The main challenges include the development of parameterizations and their incorporation into partial-waves analyses that respect the theoretical constraints and allow for a reaction-independent determination of pole positions and residues,

[1] All composite objects of quarks and gluons that are therefore subject to the strong interaction with no net color charge are called hadrons.

which uniquely characterize the properties of a given resonance. In this document we review some aspects of the theoretical and phenomenological underpinning of experimental data analyses which aim at extracting hadron resonance parameters in a controlled way.

Beyond providing a deeper understanding of the inner workings of QCD, a theoretical control over hadronic final-state interactions is also essential to employ the decays of heavy mesons for the hunt of physics beyond the Standard Model of particle physics (SM), which are driven by the electroweak interactions: in order to explain the matter–antimatter asymmetry of the universe, an amount of CP violation is necessary that exceeds that of the SM by many orders of magnitude. Thus, additional CP violation has to be present, and it has to exceed the SM predictions dramatically.

If present, CP violation in the decay of heavy mesons will show up as a complex phase, and therefore relies on interference of different amplitudes. As the observation of CP asymmetries in (partial) decay rates depends on both weak and strong phase differences, a more accurate understanding of the latter necessarily leads to an improved determination of the former, and resonating strong final states provide ideal enhancement factors for (probably very small) weak asymmetries. Therefore, the decay of a heavy meson into three or more light mesons appears to provide an ideal environment for CP studies due to the presence of a large number of meson resonances in the phase space available. Furthermore, besides enhancing the CP signals, the non-trivial distribution of the strong phase motion over the Dalitz plot allows for a test of systematics, and provides some sensitivity to the operator structure of the CP-violating source underlying the transition.

This twofold perspective of amplitude analyses should be kept in mind throughout this document: while a strong motivation clearly consists in understanding the spectrum of QCD as such, there is a strong benefit from making the results available for communities more concerned with the investigation of electroweak interactions and New Physics searches in hadronic environments.

1.1 Quark Model

[V.Mathieu, E.Santopinto]

The Quark Model was originally introduced as a classification scheme to organize the hadron spectrum. Since its introduction, significant progress has been made in the understanding of QCD, and while there is no formal relation between constituent quarks and the QCD degrees of freedom, the lattice QCD hadron spectrum closely resembles that of the quark model. In

the quark model, mesons are bound states of a valence, constituent quark and antiquark, while baryons contain three quarks. Quantum numbers of quark model bound states are obtained by combining the quantum numbers of the individual quark constituents, *e.g.* their spins and angular momenta. For example, the meson spin J is given by the vector sum of quark–antiquark spin s and orbital angular momentum l. Meson parity P and, for neutral states, charge conjugation C are given by $P = (-1)^{l+1}$, $C = (-1)^{l+s}$, respectively. It thus follows that certain combinations of total spin J^{PC}, 0^{--}, 0^{+-}, 1^{-+}, 2^{+-}, 3^{-+}, ..., do not correspond to a quark–antiquark pair. These are referred to as *exotic*. There are no exotic baryons in a corresponding sense, *i.e.* three quarks can be combined to give any combination of a half-integer spin and parity. In addition, taking into account quark flavors the quark model arranges hadrons into flavor multiplets with mass degeneracies broken by the the quark masses.

The classification of the well-established light mesons according to the quark model is summarized in Table 1.1 taken from the Review of Particle Physics [1]. Indeed, most of the observed resonances fit into the quark model pattern, although several states including the ρ_2 or the b_3 are missing. There are also well-established resonances that do not fit the quark-model classification. These include in for example states with $J^{PC} = 0^{++}$ quantum numbers, *e.g.* the the $f_0(500)$.

Hadron resonances can also be classified by the Regge trajectories they belong to. For example, for mesons, Regge trajectories are labeled by signature $\tau = (-1)^J$, naturality $\eta = P(-1)^J$, and also by isospin I and $G-$parity $G = C(-1)^I$. The absence of isospin $I = 2$ resonances implies degeneracy between Regge families, as we will discuss further in Sec. 3.3.

1.2 Lattice QCD and the hadron spectrum

[J.Dudek]

Lattice QCD is a first principles numerical approach to QCD which considers the field theory evaluated on a finite grid of points. Supercomputers are used to Monte-Carlo sample a finite, but large, number of gluon field configurations according to their importance in the QCD Euclidean path integral. Color-singlet correlation functions can then be computed using this ensemble of configurations, with the mean and variance over the ensemble providing an estimate and an uncertainty. The discrete spectrum of eigenstates of the theory can be extracted from the time-dependence of correlation functions.

In principal this is a systematically improvable approach to QCD. Calcu-

$n^{2s+1}\ell_J$	J^{PC}	$I=1$	$I=1/2$	$I=0$	$I=0$	
1^1S_0	0^{-+}	π	K	η	η'	$R2$
1^3S_0	1^{--}	$\rho(770)$	$K^*(982)$	$\omega(782)$	$\phi(1020)$	$R1$
1^1P_1	1^{+-}	$b_1(1235)$	$K_1(1400)$	$h_1(1170)$	$h_1(1380)$	$R2$
1^3P_0	0^{++}	$a_0(1450)$	$K_0^*(1430)$	$f_0(1370)$	$f_0(1710)$	$R4$
1^3P_1	1^{++}	$a_1(1260)$	$K_1(1270)$	$f_1(1285)$	$f_1(1420)$	$R3$
1^3P_2	2^{++}	$a_2(1320)$	$K_2^{**}(1430)$	$f_2(1270)$	$f_2'(1525)$	$R1$
1^1D_2	2^{-+}	$\pi_2(1670)$	$K_2(1770)$	$\eta_2(1645)$	$\eta_2(1870)$	$R2$
1^3D_1	1^{--}	$\rho(1700)$	$K^*(1680)$	$\omega(1650)$		$R4$
1^3D_2	2^{--}		$K_2^*(1820)$			$R3$
1^3D_3	3^{--}	$\rho_3(1690)$	$K_3^*(1780)$	$\omega_3(1670)$	$\phi_3(1850)$	$R1$
1^1F_3	3^{+-}					$R2$
1^3F_2	2^{++}		$K_2^*(1980)$	$f_2(1910)$	$f_2(2010)$	$R4$
1^3F_3	3^{++}		$K_3(2320)$			$R3$
1^3F_4	4^{++}	$a_4(2040)$	$K_4^{**}(2045)$		$f_4(2050)$	$R1$

Table 1.1: Well-established mesons classified according to the quark model. Duality, see Sec. 3.3, predicts the existence of four different Regge families denoted by $R1, \ldots, R4$. Resonances belonging to the same family lie on the same Regge trajectory.

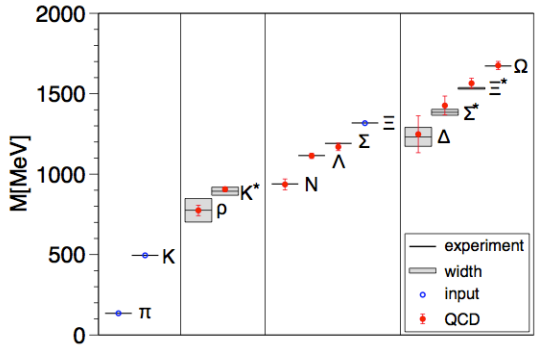

Figure 1.1: The light hadron spectrum of QCD computed using lattice techniques in [2].

lations can be performed for a range of lattice spacings, a, and an extrapolation $a \to 0$ performed. Similarly the behavior with increasing finite volume can be studied. In practice, the low mass of the physical u and d quarks provides a challenge—the numerical algorithms used to generate gluon field configurations and to compute quark propagation scale badly with decreasing quark mass. Furthermore, since very light quarks imply very light pions with large Compton wavelengths, there is a need to increase the size of the lattice volume as the quark mass decreases. For fixed lattice spacing this requires more points in the grid and thus increased computation time.

For relatively simple quantities like the masses of the lightest stable hadrons, precision calculations considering all the above systematic variations have recently been carried out. An example is presented in Fig. 1.1. In the case of *excited* hadrons, the state of the art is not yet at this level, with calculations typically being performed at a single (albeit small) lattice spacing, and with light quark masses chosen to be somewhat above the physical value. Fig. 1.2 presents an example of recent progress in determining the excited isoscalar and isovector meson spectrum. This calculation has approximately physical strange quarks but light quarks somewhat heavier than physical such that the pion has a mass of 391 MeV [3, 4, 5].

Fig. 1.2 shows a detailed spectrum of excited states of various J^{PC}, with many of the observed experimental systematics being reproduced, as well as those of the $n\,^{2S+1}L_J$ $q\bar{q}$ quark model. A clear set of exotic J^{PC} states are extracted with the isovector spectrum featuring a lightest 1^{-+} roughly 1.3 GeV heavier than the ρ meson. Slightly heavier than the 1^{-+} is a single 0^{+-} state and two 2^{+-} states, and these observations have been shown to be robust with increasing quark mass. Examination of the type of quark-gluon operator constructions which have large overlap with these exotic states suggests that they are hybrid mesons with $q\bar{q}$ in a color octet coupled to a chromomagnetic gluonic excitation. Such a construction can also generate non-exotic hybrid mesons, and indeed such states with $J^{PC} = 0^{-+}$, 2^{-+}, and 1^{--} are identified in the calculation (highlighted in orange in Fig. 1.2).

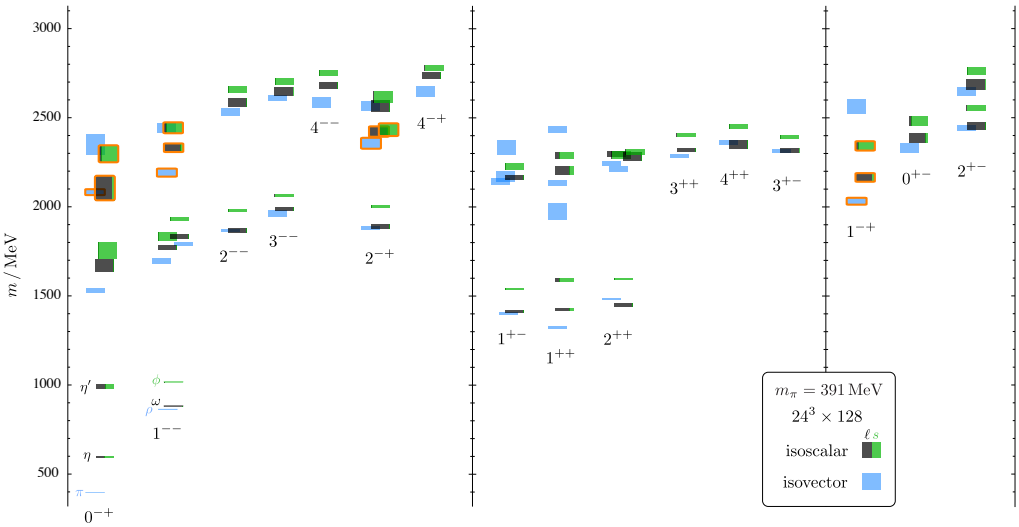

Figure 1.2: Isoscalar and isovector meson spectrum determined in a lattice QCD calculation with $m_\pi = 391\,\mathrm{MeV}$. [3].

Calculation in the charmonium sector [6] shows similar conventional meson and hybrid meson systematics.

The baryon spectrum has been computed using related techniques [7, 8]. Hybrid baryons, which cannot have exotic quantum numbers, have been predicted [9] with a quantum number distribution and operator overlaps that suggest the same chromomagnetic gluonic excitation is at work.

Computing the spectrum of glueballs is relatively straightforward within the pure-glue theory where the existence of quarks is ignored. Glueball operators can be constructed out of gluon fields and the spectrum extracted from correlation functions. The spectra so determined in [10, 11] show that the lightest glueballs have non-exotic J^{PC} with a lightest 0^{++} and somewhat heavier a 2^{++} and a 0^{-+}. However in QCD, with quarks, these glueball basis states should appear embedded within a spectrum of isoscalar mesons, possibly strongly mixed with $q\bar{q}$ basis states. Such calculations have proven to be very challenging, for example the calculation in [3] was not able to observe any states having strong overlap with glueball operators, which produced statistically noisy correlation functions. In short the role of glueballs in the meson spectrum has not been determined in lattice QCD.

Returning to Fig. 1.2, although a lot of the correct physics is present, including annihilation of $q\bar{q}$ pairs and the corresponding mixing of hidden-light and hidden-strange configurations, the calculations are clearly not complete. Most of the states extracted should in fact be unstable resonances decaying into multi-meson final states. In fact, within a finite-volume theory, there cannot be continuum of multi-meson states, rather there must be a discrete

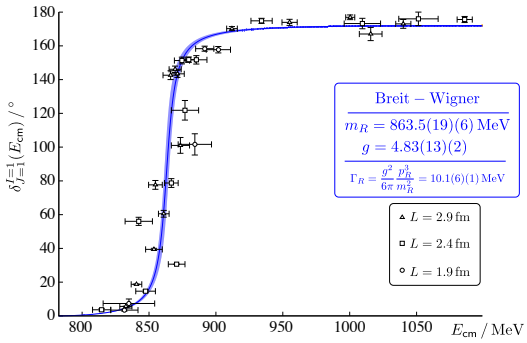

Figure 1.3: The isospin 1, P-wave $\pi\pi$ scattering phase shift determined from the discrete spectrum in three different lattice volumes. Calculation performed with quark masses such that $m_\pi = 391\,\text{MeV}$. [19]

spectrum and the volume-dependence of this spectrum can be mapped onto hadron scattering amplitudes [12, 13, 14, 15, 16, 17, 18]. The full richness of this spectrum was not resolved in [3] as only quasi-local $q\bar{q}$-like operator constructions were used, and these have very poor overlap onto multi-meson states.

The current frontier in lattice QCD calculations of hadron spectroscopy involves the inclusion of operators which efficiently interpolate multi-meson states and the extraction of the complete discrete spectrum of states in a finite-volume. An example of what can currently be achieved is presented in Fig. 1.3. By computing the complete low-energy spectrum of states with isospin 1 in multiple finite-volumes, and applying the finite-volume formalism [12, 13] to determine the elastic P-wave scattering phase shift, a rapid rise characteristic of a resonance can be observed. Fitting the phase shift with a simple Breit-Wigner form yields an estimate of the ρ resonance mass and width in a version of QCD where the pion mass is 391 MeV [19]. Ongoing calculations are addressing higher resonances which can decay into multiple channels, with additionally much work being done to develop formalism to deal with three-body and higher scattering in finite volume [20, 21].

In the near future we envisage the possibility of using the same scattering amplitude parameterizations to describe experimental data and the finite-volume spectra of QCD computed using lattice techniques.

2 Experiments

There are number of hadron programs in operations now and several are expecting for the near future. The JLab12 upgrade with two new detectors GlueX and CLAS12 foresees a dedicated program of spectroscopy with the aim of finding sub GeV hybrids. We can expect in the future further results from e^+e^- machines LHCb, SuperBelle, BES. We have the renascence of antiproton facility with FAIR (PANDA) at Darmstadt where the antiproton storage ring has been designed primarily for hadron spectroscopy

The specifications for the next generation experiment in hadron spectroscopy are: hermetic detectors for both charged and neutral particles, with excellent resolution and particle identification capability; beam energy high enough to have a sufficient phase space for the production; high statistics are needed together with sensitivity to production cross sections at the sub-nanobarn level; network work for the development of common analysis tools.

The type of reactions used of investigations of hadron spectrum can be broadly classified as: direct production quasi-elastic or diffractive production and annihilation reactions.

2.1 Baryons and direct channel production: CLAS, ELSA, MAMI, Spring-8

Low energy, elastic or quasi-elastic meson nucleon scattering are key to baryon spectroscopy. In this kind of production, also denoted $s-$channel production, the beam and the target merge to produce the resonance. Since targets are mainly nucleons, resonances studied in direct channel production are baryons excitations.

Most of our knowledge on N^* and Δ resonances stems from direct production in elastic and inelastic πN scattering experiments from more than 30 years ago. Phase shift analysis in the elastic region is a well-defined procedure that yields the scattering amplitude from the experimental data with only a few discrete alternative solutions. As the elastic pion-nucleon scattering is still the best way for precise partial-wave analyses. Availability of secondary hadron beams, *e.g.* at JPark or EIC would be required to further improve the data set. Fortunately in the last 20 years the electron accelerators *e.g.* at JLab, ELSA, MAMI, have considerably improved and new detectors and targets have been designed and went in operation. We are now in a situation, where the photo- and electro-production of pseudoscalar mesons carry the highest potential to investigate the baryonic spectrum. In addition to the resonance positions and strong residues, which describe couplings to decay channels, the electromagnetic couplings and transition form factors are being investigated. The data taken at JLab, in particular with the HD-ICE target, will provide information on the γ-neutron couplings of excited states. Also ELSA and MAMI will provide a good double polarization data. As data

stems from the neutron bound in the deuteron, one has to undertake extra effort to unfold the desired multipoles from deuteron effects, such as Fermi motion, double scattering, and other nuclear effects. For today, the experimental information on the reactions on the proton is substantially larger then that on the neutron (15% of the full $\gamma N \to \pi N$ database) especially for polarized experiments (17% of the neutron database). Only with good data on both proton and neutron targets, one can hope to disentangle the isoscalar and isovector electromagnetic couplings of the various N^* and Δ^* resonances, as well as the isospin properties of the non-resonant background amplitudes. The SAID group[1] at Georges Washington University has made much progress in this direction.

The cleanest possibility for direct baryon production is photo-production of single pseudoscalar mesons as π, η, K and η' off the nucleon. In addition $\pi\pi$ photo-production is an important channel that couples strongly to many baryon resonances. Single pseudoscalar meson photo-production is described by a set of only 4 transition amplitudes [22] (invariant, spin, transversity or helicity amplitudes). Near threshold low energy theorems are very for charged pion production and up to about 500 MeV photon energy, the Watson theorem due to two-body unitarity gives a very important constraint. Strictly this is violated already at the $\pi\pi$ threshold but it can be extended well above until the region of the Roper, the second nucleon resonance.

There exist a well established analysis procedure that allows to analyze partial-wave amplitudes directly from the data. It is a truncated partial-wave analysis, where t-channel and u-channel exchanges with poles close to the physical region can give rise to higher partial waves, and may be treated in terms of Reggeon amplitudes. For photon laboratory energies up to about 1 GeV typically only a few ($\ell_{max} = 3$) *e.g.* S-, P-, D-, and F-waves need to be included. For lower energies, *e.g.* up to 500 MeV already S- and P-waves can be sufficient, which was successfully applied in the 80s by the Kharkov/Lebedev group. With modern accelerators and detectors a much higher statistics can be reached, so that also in this region a truncation with $\ell_{max} = 2$ should be aimed.

This procedure has been used in the past successfully in fits to πN, KN and data. The powerful technique of finite energy sum rules provides further constraints between the background, Reggeon exchange and low-spin resonance amplitudes. Recent amplitudes parametrized by Regge exchanges at hight energy can be found in Ref. [23, 24, 25, 26, 27, 28, 29, 30, 31] for photo-production and in Ref. [32, 33] for pion beam. One has to be careful however when using the Regge parametrizations of the latter references. Couplings may have unphysical values since no particular care about factorability of

[1] http://gwdac.phys.gwu.edu

the residues were taken nor about exchange degeneracy constraints (see next section). Ref. [34, 35, 36] describe the data in the resonance region with an isobar model.

2.2 Mesons: JLab12, COMPASS

Beside direct production of baryon resonances, JLab hosts experiment devoted to meson spectroscopy produced peripherally. The search for mesons with exotic quantum numbers is the primary aim of the GlueX experiment at a future 12 GeV upgrade of Jefferson Laboratory, a $300M project with the first physics results in 2014. The GlueX experiment will map out the meson spectrum with unprecedented statistics using photo-production, which is a complementary reaction mechanism to other, studied so far (which include hadro-production with pion, kaon, or proton beams, or heavy meson decays). With 9 GeV photons the mass range extends up to 2.5–3 GeV and will cover the region where the light exotic multiplet is expected. A complementary meson spectroscopy program will be carried at the Hall-B with the new CLAS12 detector. The technique, electro-production at very low Q^2 (0.01–0.1 GeV^2) provides a high photon flux and a high degree of linear polarization and represents a competitive and complementary way to study the meson spectrum and production mechanisms with respect to real photo-production experiments. After a calibration period, the detector will begin to record data in 2015. Both GlueX and CLAS12 physics programs will start in conjunction with the analysis of the golden channels $\eta\pi$, $\eta'\pi$ and 3π for the detection of hybrid mesons. A detailed theoretical study on these channels is then required in the near future for the success of these experiments. Fig. 2.1 presents a typical moments analysis of data recorded by the Clas detector for $\pi^+\pi^-$ peripherally produced.

COMPASS is a high-energy physics experiment at the Super Proton Synchrotron at CERN in Geneva. One of the purposes of this experiment is the study of hadron spectroscopy with high intensity hadron beams. COMPASS aims, with his high statistical accuracy, to gain more insight into the new states which cannot be explained within the constituent quark model and which were interpreted as glueballs or hybrid states. This goal could not be reach without a fruitful collaboration with theorists. Data with pion and proton beams on proton target have already been collected in 2008, 2009 and 2012. COMPASS has already recorded events of various final states in 2008-2009 (110M events for 3π, 150k events for $K\bar{K}\pi\pi$, 110k events for $\eta'\pi$, 35k events for $\eta\pi$, etc.). This collaboration involves 250 physicists in 21 European institutions. Thanks to their accuracy, COMPASS will improve our

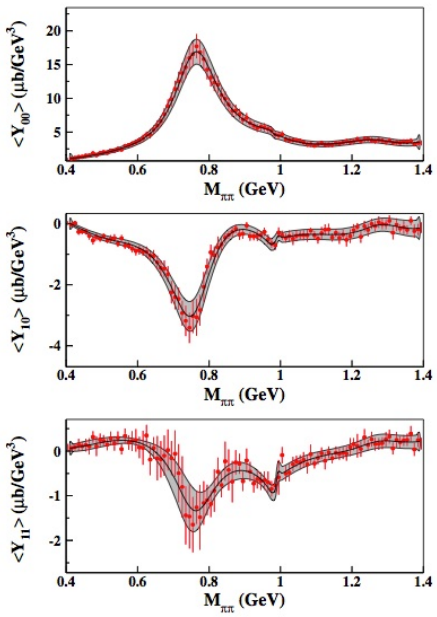

Figure 2.1: $\pi^+\pi^-$ invariant mass for the reaction $\gamma p \to \pi^+\pi^- p$ for a photon energy range $3.0-3.8$ GeV. Data were collected with the CLAS detector at the Thomas Jefferson National Accelerator Facility.

The moment $\langle Y_{00}\rangle$, corresponding to the differential production cross section $d\sigma/dtdM$, shows the dominant $\rho(770)$ meson peak. In the $\langle Y_{10}\rangle$ and $\langle Y_{11}\rangle$ moments, the contribution of the S-wave is maximum and enters via interference with the P-wave. In particular, the structure at $M \sim 0.77$ GeV in $\langle Y_{11}\rangle$ is due to the interference of the S-wave with the dominant, helicity-nonflip wave $P_{m=+1}$. In the $\langle Y_{10}\rangle$ moment, the same structure is due to the interference with the $P_{m=0}$ wave, which corresponds to one unit of helicity flip. A second dip near $M = 1$ GeV is clearly visible and corresponds to the production of a resonance that we interpret as the $f_0(980)$ [37].

knowledge on meson spectroscopy and will set up on the existence or the absence of exotic hadrons. Its goals could be only achieved by mean of an active collaboration with theorists, *i.e.* by matching their data with theoretical predictions. This collaboration should be set up in the near future to be optimal.

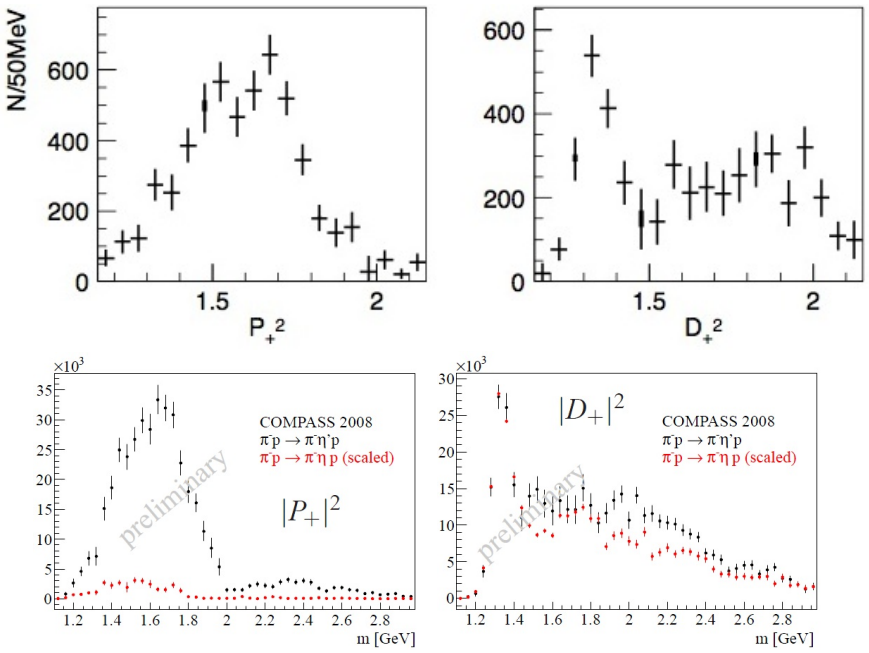

Figure 2.2: P_+ and D_+ intensity for $\eta'\pi$ invariant mass at VES (top) [38] and COMPASS (bottom) [39] . The peak around 1.3 GeV in the D_+ wave correspond to the $a_2(1320)$. The broad structure in the exotic P_+ wave could host a hybrid meson but a detailed amplitude analysis is required.

2.3 Annihilation reactions: BES-III, VEPP, PANDA

Annihilation of e^+e^- and $p\bar{p}$ have been a relatively recent addition to the host of reactions in hadron spectroscopy. The early experiments in the SLAC-LBL e^+e^- storage ring (SPEAR) produced many of the first measurements in the charmonium spectrum. They were followed by CLEO, BES, Babar with Belle, BES-III and VEPP still in operation. Charmonium decay data sets have been supplemented by the bottomonium decay data and open flavor D and B meson decays. Proton-antiproton annihilation was studied at the Low Energy Antiproton Ring (LEAR) at CERN and new experiments at center

of mass energy above charm threshold are plans for the FAIR facility.

Decays of heavy flavors are not only a source of light hadrons but are a primary source of information on the weak sector. During the B-factory age, the program to extract weak interaction parameters (as the CKM matrix elements) or to study New Physics effects went through the analysis of decays with final states with at least three particles. Final state interactions can share light at any new physics at distance scales much shorter then those of strong interactions. Light hadron final state interactions bring in phases, which interfere with the weak phases and have to be included in amplitude analysis. For example $D^0 \to K_s\pi\pi$ amplitude depends on the week CKM phase γ which can only be extracted if the strong $K\pi$ and $\pi\pi$ phases are known [40, 41].

It should be noted that in principle the same amplitude analysis tools applied to beam or target fragmentation can be used in the analysis of annihilation channels. Thus a comprehensive amplitude analysis efforts will serve all experiments.

Since 2010 experiments are in progress at the upgraded VEPP-2000 e^+e^- collider operated in the center-of-mass (c.m.) energy range from threshold of hadron production up to 2 GeV with two detectors, CMD-3 and SND. The goal of the CMD-3 and SND experiments is to study spectroscopy of the light vector mesons (ρ, ω and ϕ and their excitations) and measure cross sections of various exclusive channels of e^+e^- annihilation with high accuracy. Such measurements should help in clarification of the muon $g-2$ puzzle and provide detailed studies of the dynamics of the multi-hadron final states. The expected data samples should be sufficiently large for disentangling various intermediate mechanisms, as was already shown in the first high-statistics studies of the four-pion final state in e^+e^- annihilation at CMD-2 [42, 43] and τ decays at CLEO [44]. The $a_1\pi$ dominance with admixtures of the ρf_0 for the $2\pi^+2\pi^-$ and the $\omega\pi^0$ for the $\pi^+\pi^-2\pi^0$ final state discovered by CMD-2 was later confirmed by BaBar [45, 46] in a broader energy range, where the $\rho f_2(1270)$ as well as some other mechanisms were observed. A crucial issue for successful partial wave analysis is to use full information about events rather than separate invariant mass distributions only.

The VEPP-4M e^+e^- collider covers a c.m. energy range from 2 GeV to 11 GeV. It is currently operated in the charmonium family range with the KEDR detector. Successful application of two methods of the high-precision determination of the absolute beam energy, resonant depolarization and Compton backscattering, resulted in various experiments with record accuracy. Among them are measurements of the J/ψ and $\psi(2S)$ masses [47], of the total and leptonic width of the J/ψ [48], $\psi(2S)$ [49], $\psi(3770)$ [50], the D^0 and $D^\pm$ masses [51], the τ lepton mass [52] as well as a search for narrow

resonances from 1.85 GeV to J/ψ [53]. Also planned is a new measurement of R up to 8 GeV.

There has recently been a dramatic renewal of interest in the subjects of hadron spectroscopy and charm physics. This renaissance has been driven in part by experimental reports of $D^0\bar{D}^0$ mixing and the discovery of narrow D_{sJ} states and a plethora of charmonium-like XYZ states at the B factories, and the observation of an intriguing proton-antiproton threshold enhancement and the possibly related $X(1835)$ meson state at BES-II.

The BES-III experiment at BEPCII in Beijing [54], which has started operation in summer 2008, and with 1 billion J/ψ and 0.4 billion $\psi(2S)$ expected by the end of 2012 the precision spectroscopy amplitude analysis can be performed. Coupled with currently available results from CLEO-c, BES-III will make it possible to study in detail, and with unprecedentedly high precision, light hadron spectroscopy in the decays of charmonium states and charmed mesons. In addition, about 90 million $D\bar{D}$ pairs will be collected at BES-III in a three-year run at the $\psi(3770)$ peak. Many high precision measurements, including CKM matrix elements related to charm weak decays, decay constants f_{D+} and f_{D_S}, Dalitz decays of three-body D meson decays, searches for CP violation in the charmed-quark sector, and absolute decay branching fractions, if recently observed signs of mixing in the $D^0\bar{D}^0$ meson system are actually due to new physics or not. BES-III measurements of f_{D+} and f_{D_S} at the $\sim 1\%$ precision level will match the precision of lattice QCD calculations and provide the opportunity to probe the charged Higgs sector in some mass ranges that will be inaccessible to the LHC. With modern techniques and huge data samples, searches for rare, lepton-number violating, flavor violating and/or invisible decays of D-mesons, charmonium resonances, and tau-leptons will be possible. Studies of τ-charm physics could reveal or indicate the possible presence of new physics in the low energy region.

PANDA is one of the major projects at the FAIR-Facility in Darmstadt. FAIR is an extension of the existing Heavy Ion Research Lab (GSI) and is expected to start its operation in 2015. PANDA studies interactions between antiprotons and fixed target protons and nuclei in the momentum range of 1.5-15 GeV/c using the high-energy storage ring HESR. The PANDA collaboration with more than 450 scientists from 17 European countries intends to do basic research on various topics around the weak and strong forces, exotic states of matter and the structure of hadrons.

2.4 Prospects at the LHC: LHCb

The LHCb experiment [55] is designed to exploit the huge $b\bar{b}$ cross section at pp collisions at LHC energies [56] for precision flavour physics. The same characteristics that optimize LHCb for b physics, also make it an excellent charm physics experiment, benefiting from a charm cross section of (6.10 ± 0.93) mb in 7 TeV proton-proton collisions [57]. This leads to enormous, and still growing data sets of beauty and charm hadrons, with tens of millions of cleans signal events collected already in many charm decays. Such high-statistics data samples constitute an huge opportunity for high precision flavour physics but they also challenge the theoretical tools we have to analyze these datasets, including partial-wave analyses.

One of the key aims of LHCb is the precision measurement of CP violating parameters in a wide variety of decay modes to thoroughly over-constrain the Standard Model description of CP violation and quark transitions, with high sensitivity to physics beyond the Standard Model. CP violation in the Standard Model is due to CP violating phases in weak interactions. Amplitude/partial-wave analyses are intrinsically sensitive to phases and a powerful tool for CP violation measurements. They are used extensively at LHCb. Below we discuss two classes of such analyses—those that use helicity amplitudes to separate different angular momentum and thus different CP states on one hand, and Dalitz analyses and their generalizations on the other.

The time-dependent amplitude analysis of the decay $B_s \to J/\psi KK$ allows the measurement of the CP violating phase ϕ_s. This phase is precisely predicted in the Standard Model: $\phi_s^{SM} = -0.036 \pm 0.002$ [58]. A precision measurement of this phase is therefore highly sensitive to contributions from physics beyond the Standard Model, which could for example enter in the loop diagram mediating B_s mixing. An amplitude analysis is required to disentangle the odd and even CP components of the final $J/\psi KK$ state, which is composed of the three angular momentum states of the dominant $J/\psi\phi$ contribution and the $J/\psi\{KK\}_{S-wave}$ amplitude. The topologically similar but less abundant decay $B_s \to J/\psi\pi\pi$ is dominated by the CP odd contribution [59], which makes the extraction of ϕ_s simpler. A combined analysis of these decays yields $\phi_s = 0.07 \pm 0.09(\text{stat}) \pm 0.01(\text{stat})$ [60], which is by far the word's most precise measurement of this quantity.

Dalitz analyses and their generalizations are an important tool for LHCb's precision measurements both in charm [61, 62, 63, 61] and in B decays [64, 65, 59, 66, 67, 68]. One of the biggest problems in exploiting the full potential of this tool for precision CP violation measurements is the amplitude model uncertainty. For this reason, LHCb makes widespread use model-

independent approaches. In this context, input from charm factories, which provide access to both magnitude and phase information across the Dalitz plot in a model-independent way [69, 70, 71, 72], can significantly improve measurements at LHCb. This is especially the case for the measurement of the key *CP* violation parameter γ in $B^{\pm} \to DK^{\pm}$ and related decays. This type of analysis depends on the amplitude structure of the subsequent D decay. Model-independent input from CLEO-c [73, 74, 75] is used at LHCb for $B^{\pm} \to DK^{\pm}$ with $D \to K_S\pi\pi$, $D \to K_S KK$ and $D \to K\pi\pi\pi$ [76, 64, 77, 65]. However, such input is not available for all interesting decay modes (see for example $B^{\pm} \to DK^{\pm}$ with $D \to KK\pi\pi$ [78]), and for others the statistical precision is limited [73]. The BES-III collaboration has already recorded more than three times as much data as CLEO-c at the charm threshold [79]. BES-III will therefore be able to increase the precision and scope of these measurements significantly, which will have a large impact on the eventual precision that can be reached at LHCb, or its upgrade, in this important class of analyses. Nevertheless, it would be highly desirable not to be restricted to decay modes and analyses where such model-independent input exists. Reliable, theoretically motivated, and practically usable amplitude models, with components that can be safely transferred across analyses and decay modes, would be of enormous benefit to LHCb and future high-precision flavour physics experiments such as BELLE II the LHCb upgrade.

3 Amplitude Analysis

[C.Hanhart]

Hadron spectroscopy aims at the identification of hadron resonances and the determination of their properties. In the limit of large number of colors, hadrons become bound states of constituent quarks. In reality, almost all of them are resonances that decay strongly to ground state hadrons—pions, kaons, etas, and nucleons. The heavier the resonance, the more multi-particle channels are allowed kinematically as final states. As a result, resonances become broad, overlap, and their identification gets increasingly difficult. The goal of the amplitude analyses outlined here is to pin down the spectrum in the so called resonance region which typically corresponds to excitation energies not greater than 2–3 GeV.

The easiest and most commonly used parametrization for production and scattering amplitudes is built from sums of Breit–Wigner functions (BWs) with energy-dependent widths, sometimes accompanied by (smoother) background terms. While this ansatz typically allows for a high-quality fit of many-body final states, it suffers from various problems. The poles of the BWs are in general not identical to the true poles of the S-matrix. As such their parameters may differ between different reactions, which prevents a systematic, consistent study of many final states. Sums of BWs typically violate unitarity in both scattering and production—in the former case since the optical theorem typically requires energy-dependent complex phases between the different terms, in the latter since in general Watson's theorem, which calls for the equality of scattering and production phases in the elastic regime, is violated. The standard BWs are not analytic functions and thus do not allow any access to the poles of the S-matrix.

In this section we outline theoretical aspects that need to be considered to arrive at parametrizations of amplitudes that try to minimize the effect of the above-mentioned problems.

From the point of view of reaction theory, also known as S-matrix theory, resonances are poles of partial-wave scattering amplitudes in the unphysical domain of kinematical variables, energy, and/or angular momenta. Thus, their identification requires a complex amplitude analysis. S-matrix theory imposes severe constraints on the amplitudes allowed, such as unitarity, analyticity, as well as crossing symmetry. In addition, the amplitudes have to be consistent with the assumed discrete symmetries of the underlying theory. Depending on the kinematical regime of an experiment different aspects of this list may become relevant. For example, low-energy scattering is dominated by a few elastic partial waves, which may be constrained by unitarity, analyticity, and in some special cases crossing symmetry (cf. Sec. 3.1 on dispersion theory). To control subleading singularities, or if there is not sufficient information about particle scattering available to employ dispersion theory, in addition to the general principles, it is sometimes necessary to impose further properties on the reaction dynamics, e.g. from long-ranged meson

exchanges whose strength may be constrained from data (e.g. the strength of the pion exchange in $\pi\rho \to \rho\pi$ is given by the width of the ρ-meson) or by chiral symmetry (cf. Sec. 3.2 on dynamical coupled-channel methods and related approaches). On the other hand, a detailed understanding of resonance production with high-energy beams may require knowledge of singularities in the complex angular momentum plane—Reggeons (cf. Sec. 3.3 on duality and finite energy sum rules).

In general, amplitude analysis can be considered as a three-step process. In step one, theoretical amplitudes are proposed and constrained by fitting the experimental data. In step two, these amplitudes are tested against various constraints that are used to minimize the amount of unresolved ambiguities in the amplitude determination. Finally in step three, the amplitudes are extrapolated (analytically continued) to the unphysical kinematical region of energy and angular momentum to determine properties of resonances.

With the advent of new high statistics experiments, together with the development of theoretical tools the widely used isobar model could now be replaced by model independent analyses. Connecting the emerging lattice results with the parameters extracted using the analysis techniques mentioned above will provide a direct contact between experimental data and QCD.

3.1 Dispersive methods

[C.Hanhart, M.Hoferichter, B.Kubis]

In this section we will discuss several examples where dispersion relations (DRs) have been applied with the aim of obtaining precision parameterizations of amplitudes at low energies and performing their analytic continuation. Another important aspect that concerns the connection of low-energy physics and the high-energy region within dispersion theory will be touched upon in Sec. 3.3.

A resonance is uniquely characterized by its pole and residues, the position of the pole being universal, its residues depending on the decay channel in question. The challenge in the precision determination of these parameters lies in the restriction that experiments are limited to real, physical values of the center-of-mass energy s. In principle, DRs provide a rigorous way of analytically continuing amplitudes from the physical regime into the complex plane, and thus of unambiguously extracting the pole parameters of the resonance. Only when a resonance is well isolated from others and is also far from thresholds, one can use simple expressions like Breit–Wigner amplitudes that provide, in a limited region, a very good approximation to the result one would obtain from dispersion theory. Mathematically, these are

cases where the distance of the resonance pole to the real axis is smaller than its distance to any other singularity, or where there is just one threshold cut nearby. Resonances corresponding to such a situation have been thoroughly studied and their properties are well established. Nowadays we are trying to understand the complicated part of the spectrum, where this ideal situation often does not occur and resonances are wide, with poles relatively deep in the complex plane. Effects of overlapping resonances and proximity to more than one threshold due to many possible decay channels require more elaborate techniques.

For a general introduction to dispersive techniques, we refer to Refs. [80, 81, 82]. Briefly, in terms of physics, DRs are a consequence of causality, which mathematically allows us to analytically extend the amplitudes into the complex plane, and then use Cauchy's theorem to relate the amplitude at any value of the complex plane to an integral over the (imaginary part of the) amplitude evaluated on the real axis, where data are available. Such a relation can be used in several ways. On the physical real axis, it implies that the amplitude has to satisfy certain integral constraints. Thus, one can check the consistency, within uncertainties, of the data at a given energy against the data that exist in other regions. Additionally, DRs may be imposed as constraints, by forcing the amplitude to satisfy the DR while fitting the data. Finally, certain sets of coupled DRs are so strongly constrained (see the discussion of Roy equations below) that they can actually be *solved* as a boundary problem in a limited (typically low-)energy range, given a specific high-energy input and depending on a well-defined number of parameters (subtraction constants) [83, 84, 85, 86].

Especially, one can even use a DR to obtain values for the amplitude at energies where data do not exist, using existing data in other regions. Once one has an amplitude that satisfies the DR and describes the data well, it is possible to extend the integral representation to obtain a unique analytic continuation into the complex plane (or at least to a particular region of the complex plane where the validity of the DR can be rigorously established). For partial-wave amplitudes, one can thus study the complex-energy plane and look for poles and their residues, which provide the rigorous and observable-independent definition for the resonance mass, width, and couplings.

Prime examples for precision determinations of resonance pole positions by dispersive techniques concern the σ or $f_0(500)$ [87, 88] as well as the κ or $K_0^*(800)$ resonance [89]. While both are still "simple" in the sense that they are overwhelmingly dominantly *elastic* resonances (in $\pi\pi$ and πK scattering, respectively), their poles are non-trivial to determine since they lie far away from the real axis, with widths of about 550 MeV in both cases.

By convention, the width Γ of a resonance is defined as $\Gamma = -2\,\mathrm{Im}\sqrt{s_p}$, where s_p denotes the complex pole position of the resonance. The (complex) range of validity of the corresponding DRs is restricted by the singularities of the so-called double-spectral region, as well as by the requirement of the partial-wave projection to converge, and can be shown to still comprise the poles under investigation. One furthermore employs the consequence of unitarity that poles on the second Riemann sheet correspond to zeros on the first sheet; the positions of the latter are determined in practice. As the partial waves in these cases are given by DRs using imaginary parts along the real axis only, with kernel functions known analytically, this procedure is then straightforward.

DRs have been extensively studied for various $2 \to 2$ reactions, with a few extensions to include more complicated final states [90]. Amplitudes for two-body reactions depend on the Mandelstam variables s and t (or u), which are related to center-of-mass energy and momentum transfer, respectively. Typically, DRs are formulated in terms of s, with the t-dependence either fixed or integrated over. The former are referred to as "fixed-t DRs." Of special importance among these kinds of DRs is the case $t = 0$ for elastic reactions, known as "forward DRs," since, due to the optical theorem, the imaginary part of the forward amplitude is proportional to the total cross section, and data on total cross sections are generically more abundant and of better quality than on amplitudes for arbitrary values of s and t.

On the other hand, one can eliminate t by projecting the amplitude onto partial waves, for which then a DR is written. The advantage of these partial-wave DRs is that their poles on the second Riemann sheet are easily identified as resonant states with the quantum numbers of the partial wave. Therefore, they are very interesting for spectroscopy. However, due to crossing symmetry, partial waves have a left-hand cut in the unphysical s region, which also contributes to the DR. If the region of interest lies very far from this cut, it can be neglected or approximated, but when closer, or if one wants to reach a good level of precision, it becomes numerically relevant and has to be taken into account. Since the amplitude in the unphysical region may correspond to different processes arising from crossed channels in other kinematic regions and other partial waves, this complicates the construction of DRs substantially. Dealing rigorously with the left-hand cut usually involves an infinite set of coupled integral equations, known for $\pi\pi$ scattering as Roy equations [91], but other versions exist for $\pi K \to \pi K$, $\gamma\gamma \to \pi\pi$, and $\pi N \to \pi N$, under the generic name of Roy–Steiner equations [92, 93]. There is a considerable and relatively recent progress, as well as growing interest in obtaining rigorous dispersive descriptions of these processes [85, 94, 95, 96, 97, 86, 98, 99, 100, 101, 102], which play an essential role

when describing final states of almost all other hadronic strongly interacting reactions.

In all these variants of DRs the integrals formally extend to infinity. In order to achieve convergence and also to suppress the high-energy contribution, one introduces so-called subtractions. In a subtracted version of a given DR, the integrand is weighted by additional factors of $1/(s - s_0)$, where s_0 is referred to as the subtraction point, at the expense of introducing a priori undetermined parameters (subtraction constants). For a $2 \to 2$ scattering process in general two subtractions are required to ensure convergence [103, 104], but once or even less subtracted relations exist for certain amplitudes. Subtraction constants can be constrained by matching to effective field theories, lattice calculations, or simply fits to data. For the high-energy region one typically makes use of Regge theory, which is known to describe data on, for instance, total cross sections up to very large energies well. Even if data are not very precise or non-existent, Regge theory allows for predictions for different processes by combining the results for well established reactions by means of factorization. Regge predictions are less robust for the t-dependence of the amplitudes, although if only small t are required, they provide a reasonable approximation. Simple and updated Regge parametrizations can be found in the Review of Particle Physics [1], except for meson–meson scattering for which we refer to [105, 97, 106, 107].

Since most hadronic observables involve pions, kaons, or light nuclei in the final state, at some stage their theoretical description requires input from elastic $\pi\pi$, πK, and πN scattering via the so-called Fermi–Watson theorem [108, 109]. For processes with only two strongly interacting final-state particles, it fixes the phase of the whole amplitude to that of the hadron pair. A rigorous dispersive implementation of this theorem can be achieved via the Muskhelishvili–Omnès (MO) method [110, 111], where the amplitude is expressed in terms of an Omnès factor uniquely determined by the phase of the scattering process of the final state. This method is particularly well-suited for the study of meson form factors, not only pion, kaons, but charmed D-mesons as well, see for instance [112, 113, 114, 115, 116, 117, 118] and references therein. In addition to the right-hand cut accounted for by the MO method, the description of production amplitudes involves a left-hand cut. It should be stressed that the structure of this left-hand cut is different from the left-hand cut of the pertinent scattering reaction.

Building upon MO techniques, one may obtain a consistent treatment of $\pi\pi$ rescattering for more complicated reactions as well, e.g. using Khuri–Treiman techniques for three-particle decays [119]. If for a given decay the contribution from the left-hand cut is known to be suppressed, e.g. for $\eta, \eta' \to \pi^+\pi^-\gamma$ [120], and can be expanded in a polynomial, this setup re-

duces to the original MO solution, while otherwise coupled integral equations need to be solved. These integral equations happen to be linear in the subtraction constants, so that the full solution can be reconstructed by a linear combination of basis functions that correspond to the choice of one subtraction constant set equal to 1 and the others put to zero. In this way, one obtains a description of the amplitude in terms of a few parameters which can be determined by comparison to experiment, see [121] for the example of $\gamma\pi \to \pi\pi$. For a real decay process, the solution of the integral equations is further complicated by the analytic properties of the amplitude, which require a careful choice of the integration contour in the complex plane. For an application of these methods to $\eta, \omega, \phi \to 3\pi$ decays see [122, 123, 124, 125].

Watson's final-state theorem as well as the more general consequences thereof encoded in the use of MO and Khuri–Treiman techniques only apply in the region of *elastic* unitarity (or at least as long as inelastic effects are sufficiently small to be negligible). In principle, the MO method can be generalized to multiple coupled channels, provided the corresponding multiple-channel T-matrix is known. In practice, this has been implemented mainly for the case of the $\pi\pi$ isospin $I = 0$ S-wave, where the inelasticity sets in sharply at the $\bar{K}K$ threshold, which at the same time almost coincides with the position of the $f_0(980)$ resonance. In this case, the additional input needed beyond the $\pi\pi$ scattering phase shift are modulus and phase of the $\pi\pi \to \bar{K}K$ transition. Applications have mainly concerned scalar form factors of different kinds [126, 127, 128, 129, 130]. For the πK system, strangeness-changing scalar form factors have been studied, taking the coupling to ηK and $\eta' K$ into account [131, 132]. It needs to be said, though, that this method can be realistically applied mainly in contexts where inelasticities are dominated by one or two channels; compare also the suggestion to approximate the coupling to additional channels via resonances only [113]. The combination of the Khuri–Treiman method to treat three-body decays with inelastic channel coupling has not been undertaken to date.

For more complicated processes a rigorous formulation of DRs soon becomes extremely demanding. In such a situation, one could try to use models that incorporate at least the most relevant analytic structure, impose further constraints in the form of sum rules, and make sure that the resonances claimed lie within the applicability of the approach. Some models, based on simplified DRs, as for instance the N/D method or some unitarized models, can be very useful to obtain resonance poles and parameters in cases with coupled channels, at least in those channels where reliable data exist. By all means, one should refrain from making spectroscopic claims from simple models that fail do obey these constraints.

3.2 Dynamical coupled channels, Chew–Mandelstam, *K*-matrix, and related approaches

[M.Doering]

These well established techniques still await implementation in the analysis of modern data sets. The analysis of excited baryons could be carried out along similar lines although the phenomenology is slightly different. One complication arises from known strong inelasticities into multi-pion states, mostly $\pi\pi N$. For example, two pions with the $\rho(770)$ quantum numbers are known to be responsible for inelasticities at higher energies. The two pions and the nucleon can also be in relative S-wave, i.e. one can have the effective quantum numbers of a σN state. With the centrifugal barrier absent, this configuration leads to large inelasticities into the $\pi\pi N$ channel even at low energies, leading to the unusual resonance shape of the (very light) Roper resonance $N(1440)1/2^+$. In other words, from the standpoint of meson spectroscopy, one has maximal contamination from excited baryons, while from the standpoint of baryon analysis, the πN decay channel needs to be supplemented with three-body states.

Furthermore, a two-particle subsystem of the $\pi\pi N$ system can also contain resonance singularities. As mentioned, the $\pi\pi$ subsystem can have the quantum numbers of a $\rho(700)$, coupling to the nucleon with a certain isospin, total spin, and total angular momentum—in general, more than one configuration is possible. Those singularities lead to branch points in the complex plane of the overall center-of-mass scattering energy. These non-analyticities are located on the same sheets as resonances and can lead to false resonance signals if not properly taken into account [133]. Last but not least, the inelasticities from channels formed by a stable baryon and a stable meson are important. The prime example is the strong coupling of the ηN channel to the S_{11} partial wave, in particular the $N(1535)1/2^-$.

The complex phenomenology of the baryon resonance region has, so far, hindered the implementation of the rigorous methods discussed in the previous sections. Also, the search for new baryon resonances usually implies a multi-channel fit to data of different reactions, to look for resonances that couple only weakly to the πN channel. Recently, experimental activity has focused on photo- and electroproduction reactions, with a variety of final states such as πN, $\pi\pi N$, ηN, $\pi\eta N$, $K\Lambda$, $K\Sigma$, and ωN. As resonance pole positions are independent of the reaction studied, the simultaneous analysis of different final states facilitates the search for weak resonance signals.

Several analysis tools have been developed for the analysis of excited baryons, among them the so-called dynamical coupled channel approaches, pursued in the ANL/Osaka (former EBAC) collaboration, in the Jülich/

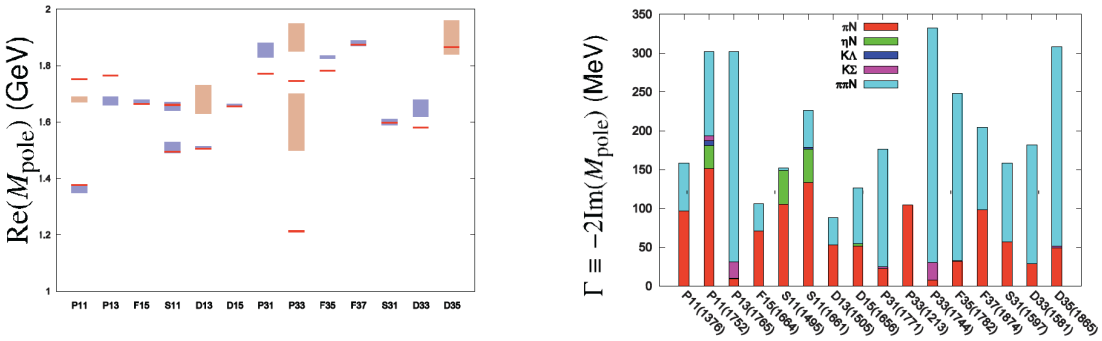

Figure 3.1: Baryon spectrum: masses (left) and widths (right) from the ANL/Osaka approach. [134].

Athens/ GWU collaboration, and in other groups [134, 135, 136, 137], see Fig. 3.1 for recent results. The left-hand cuts are approximated perturbatively by u-channel baryon exchanges, while s-channel unitarity, driven by the right-hand cut, is respected exactly. The discussed $\pi\pi N$ three-body states are included such that two-body subsystems describe the corresponding phase shifts. Subthreshold non-analyticities such as the circular cut, short nucleon cut, and further left-hand cuts are present. In the Jülich approach, the t-channel dynamics for the ρ and σ quantum numbers is provided by the use of dispersive techniques and a fit to $N\bar{N} \to \pi\pi$ data [138]. For other quantum numbers and channels, t-channel exchanges are truncated to the lightest (excited) mesons. The t- and u-channel exchanges constrain the amplitude, providing a background that connects different partial waves and limiting the room for resonances.

Another aspect of three-body dynamics is the consistent implementation of two-body decays. It has been shown [139] that unitarity in the three-body sense can be achieved by complementing three-body states with appropriate exchange processes. For example, in the three-pion system a $\pi\rho(770)[\pi\pi]$ state requires appropriate pion exchanges to fulfill unitarity. That principle has inspired the construction of dynamical coupled-channel approaches in baryon analysis as well [134, 135]. In meson analysis, three-body unitarity has been explored in [140], using effective Lagrangians and isobars, that fulfill two-body unitarity and fit the corresponding phase shifts. If, in that approach and related approaches of baryon analysis, one restricted the rescattering series to the first term, one would recover an amplitude closely related to the traditional isobar picture that may or may not be unitary in the two-body sense, but is never unitary in the three-body sense. Summing up the consistently constructed interaction beyond the leading term, including rearrangement graphs, restores unitarity in the three-body sense.

See also [141], where three-body unitarity based on point-like interactions is considered.

Coming back to the analysis of excited baryons, in dynamical coupled channel approaches, usually a scattering equation with off-shell dependence of the driving interaction is solved. If the interaction is factorized on-shell, the integral equation reduces to a matrix equation in coupled channels. Real, dispersive parts of the intermediate propagating states can be maintained. Such contributions are relevant for the reliable analytic continuation to search for resonance poles and residues. For example, in the GWU/INS (SAID) approach the interaction is parameterized in each partial wave by polynomials and without the need of explicit resonance propagators [142]. This makes this approach suited for the search of resonances, because poles are generated automatically if required by data.

If, furthermore, the real, dispersive parts are neglected, one obtains the K-matrix formulation. This is the minimal formulation in which two-body unitarity is still preserved. Currently active analysis efforts in the K-matrix formulation are pursued by the Bonn–Gatchina [143, 144] and the Gießen groups [145, 146]. Conceptually related methods are used in the MAID [147], Kent State [148], and the Zagreb [149] approaches.

In the search for excited baryons, considerable progress has been made in the analysis of the corresponding data. In particular, recent data with unprecedented accuracy from ELSA, JLab, MAMI, and other facilities have improved the precision determination of resonance parameters. Still, no consensus has been reached on the resonance content, in particular for broad resonances or those that couple only weakly to the analyzed channels, cf. Fig. 3.2. It is expected that additional constraints from crossed channels and analyticity in complex angular momenta will help improve the reliability of resonance extraction and determination of the spectrum. This is particularly relevant for the data in forward direction and at higher energies. Here, a matching of Regge amplitudes and unitary methods is a promising way to provide the correct asymptotic behavior.

Another direction in which systematic uncertainties underlying these phenomenological analyses can be quantified is to test whether the amplitudes satisfy S-matrix analyticity as expressed by finite energy sum rules (FESR). Some constraints of this type are included in the GWU/INS (SAID) approach [150]. Despite the rather involved phenomenology and the conceptual differences of the discussed baryon analysis tools, there are indications that results become eventually consistent among different groups [151], and that the long-sought determination of the baryon spectrum gets within reach.

J. Beringer et al. (Particle Data Group), Phys. Rev. D86, 010001 (2012).

Resonance	Rating	N_{pp}	Resonance	Rating	N_{pp}	Resonance	Rating	N_{pp}
$N(1440)1/2^+$	****	13	$N(1520)3/2^-$	****	17	$N(1535)1/2^-$	****	15
$N(1650)1/2^-$	****	18	$N(1675)5/2^-$	****	14	$N(1680)5/2^+$	****	17
$N(1685)$	*		$N(1700)3/2^-$	***	15	$N(1710)1/2^+$	***	14
$N(1720)3/2^+$	****	17	$N(1860)5/2^+$	**	9	$N(1875)3/2^-$	***	16
$N(1880)1/2^+$	**	20	$N(1895)1/2^-$	**	17	$N(1900)3/2^+$	***	18
$N(1990)7/2^+$	**	9	$N(2000)5/2^+$	**	11	$N(2040)3/2^+$	*	
$N(2060)5/2^-$	**	13	$N(2100)1/2^+$	*		$N(2150)3/2^-$	**	11
$N(2190)7/2^-$	****	11	$N(2220)7/2^-$	****	7	$N(2250)9/2^-$	****	
$N(2600)11/2^-$	***		$N(2700)13/2^+$	**				
$\Delta(1232)$	****	8	$\Delta(1600)3/2^+$	***	12	$\Delta(1620)1/2^-$	****	10
$\Delta(1700)3/2^-$	****	11	$\Delta(1750)1/2^+$	*		$\Delta(1900)1/2^-$	**	13
$\Delta(1905)5/2^+$	****	11	$\Delta(1910)1/2^+$	****	13	$\Delta(1920)3/2^+$	***	21
$\Delta(1930)5/2^-$	***		$\Delta(1940)3/2^-$	*	5	$\Delta(1950)7/2^+$	****	13
$\Delta(2000)5/2^+$	**		$\Delta(2150)1/2^-$	*		$\Delta(2200)7/2^-$	*	
$\Delta(2300)9/2^+$	**		$\Delta(2350)3/2^-$	*		$\Delta(2390)7/2^+$	*	
$\Delta(2420)11/2^+$	****		$\Delta(2400)9/2^-$	****		$\Delta(2750)13/2^-$	**	
$\Delta(2950)15/2^+$	**							

E.g.: V. Kuznetsov *et al.*, Phys. Lett. B **647**, 23 (2007); V. Kuznetsov *et al.*, Phys. Rev. C **83**, 022201 (2011); I. Jaegle *et al.*, Eur. Phys. J. A **47**, 89 (2011).
M. Ablikim *et al.* [BES Collaboration], Phys. Rev. D **80**, 052004 (2009).
A. V. Anisovich, R. Beck, E. Klempt, V. A. Nikonov, A. V. Sarantsev and U. Thoma, Eur. Phys. J. A **48**, 15 (2012);
N_{pp} particle properties were determined; 400 in total. Be cautious, there are ambiguities ! Promoted to three-star resonance

Figure 3.2: Baryon spectrum from the Particle Data Group with certain new states from the Bonn–Gatchina analysis [144] and others.

3.3 Duality and finite energy sum rules

[G.Fox, V.Mathieu. A.Szczepaniak]

In the preceding sections we focused on those S-matrix properties that are most important at low energies. Specifically we discussed how, at the level of partial waves, to employ analyticity in order to implement unitarity and use effective Lagrangians to implement various symmetries.

The number of relevant partial waves grows with increasing channel energy and in reactions that, at least in some channels involve large Mandelstam invariants a large (infinite) number of partial waves will contribute. As shown by Regge, high energy behavior in a direct channel is dual to resonances in overlapping crossed channels. The crossed channel resonance contributions can be expressed in terms of Regge poles and cuts, often referred to as Reggeons. The location and properties of Reggeons is constrained

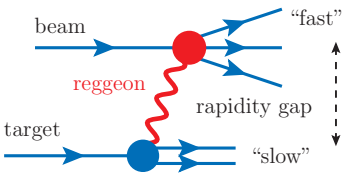

Figure 3.3: Factorization in peripheral production. The upper vertex represents beam fragmentation and is described by beam plus Reggeon scattering.

by analyticity of partial waves continued to the complex angular momentum plane.

Schematically, as a function of channel energy variable, s, reaction amplitudes can be separated into a contribution from the low-energy region, where the s-dependence can be parametrized with a finite number of partial waves, and the high-energy region, where the amplitude is determined through Reggeons. The low-energy partial waves contain information about directly produced resonances and Reggeons about resonances in crossed channels. To eliminate possible double counting, the low-energy partial waves need to be removed from the high-energy Reggeon contributions. Analyticity is then used to constrain the two regions. That is, with all other kinematical variables fixed, the amplitude is an analytical function of channel energy with singularities originating from bound states and opening of physical thresholds. This enables one to write dispersion relations that connect the low-energy partial waves with the high-energy Reggeons. The energy dependence of such DRs is often converted into a set of moments and used as sum rules, also known as finite energy sums rules (FESR) [152, 153] that relate parameters of resonances in direct and crossed channels. The classic application of FESR was in charge exchange πN scattering [154, 155], and used to establish a relation between the leading, ρ meson, and πN resonances.

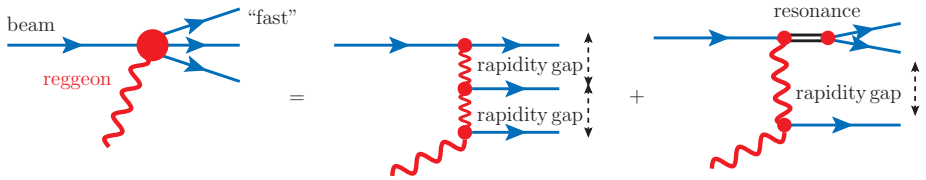

Figure 3.4: Specific, non-overlapping contributions to the Beam + Reggeon $\to$ 3 particles amplitude.

The observation that the low-energy contribution to FESR when saturated by resonances reproduces the contribution from leading Reggeons at high energy led to the concept of duality [156, 157]. According to this hypothesis directly produced resonances in low partial waves are dual to Reggeons,

and residual, non-resonant backgrounds are dual to the Pomeron. This hypothesis is consistent with what is expected in the limit of large N_c and the valence quark model. It is therefore worth noting that the existence of various exotic resonances that cannot be accommodated within the quark model would also lead to violations of this simple two-component duality. FESR studies can thus provide additional arguments in favor or against the existence of new resonances. As an example let us consider K^+p elastic scattering. Directly produced resonances manifest themselves in the large imaginary part of the amplitude. The K^+p direct channel has strangeness $+1$ and the absence of flavor exotic baryon resonances implies relations between crossed-channel Reggeons that enforce the vanishing of the Reggeon contributions to the imaginary part of the amplitude. These are known as exchange degeneracies (EXD), and in the case of K^+p involve the ρ and a_2 Regge trajectories. Similarly, the absence of isospin 2 resonances in $\pi\pi$ scattering implies EXD between the ρ and f Regge trajectories. The effect can be observed, for example, in the 3π Dalitz distribution obtained from π^- diffractive dissociation, as illustrated in Fig. 3.5 [158].

FESR can also be use to distinguish what is the background and what is a $q\bar{q}$ resonance. As illustrated in Fig. 3.6 the final-state interactions generating resonances in the low-spin partial waves in the 23 channel are dual to the ρ^0 and f in the 13 channel.

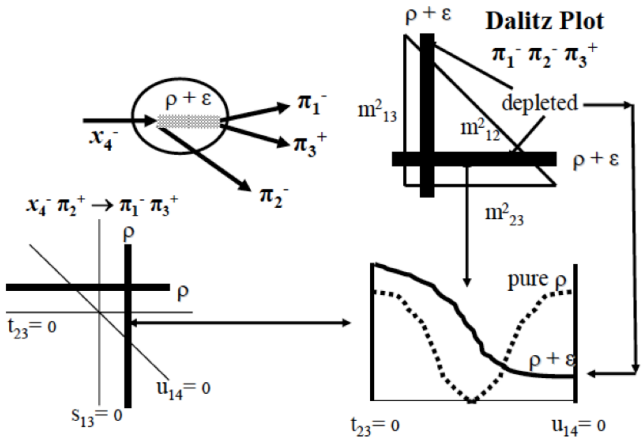

Figure 3.5: The ρ and f must interfere coherently to suppress double charge exchange in the $\pi_4^-\pi_3^- \to \pi_1^-\pi_2^-$ channel.

Exchange degeneracies between the leading Regge trajectories are satisfied to within roughly 10%, and the EXD families are indicated in Table 1.1 and Fig. 3.7. Duality therefore leads to an important constrain that helps to

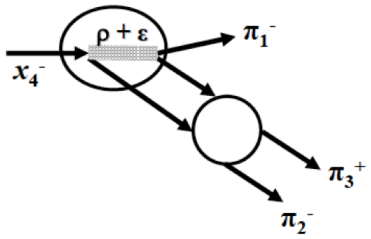

Figure 3.6: This final state interaction "generated" the Reggeons in the 23 channel and we include these in the $\rho + f$ ansatz in 13 [158].

reduce the number of parameters in amplitude parametrizations and improve the predictability of a fit.

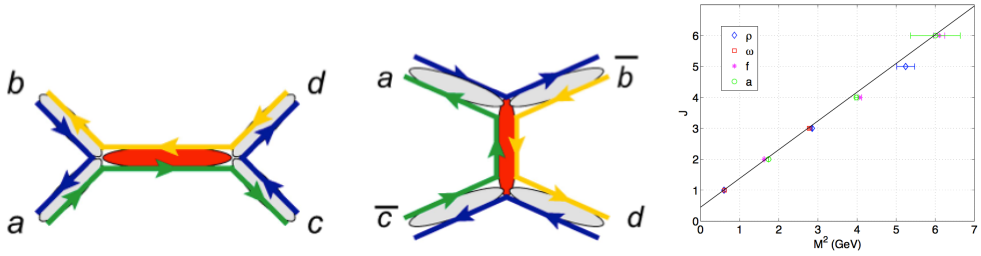

Figure 3.7: Duality hypothesis as supported by the quark model. The low-energy s-channel amplitude (left) is related to the high-energy t-channel amplitude (middle). Right: exchange degeneracy between the ρ, ω, f, and a families.

The resonance-Reggeon duality can be extend to multiparticle production as illustrated in Figs. 3.3 and 3.4. At small scattering angle, when the center-of-mass energy of colliding hadrons is significantly above the resonance region, the reaction amplitude factorizes into a product of beam and target fragmentation sub-processes mediated by the Pomeron/Reggeon exchange as depicted in Fig. 3.3. With a meson or the photon as a beam and nucleon as a target, beam fragments provide the laboratory to study meson resonances while the target fragments carry information about baryon resonances. Beam fragmentation has been the primary source of information about meson–meson phase shifts and two- and three-body resonance decays. The description of the vertex representing beam-Reggeon scattering to a few meson fragments follows the principles of resonance-Reggeon duality. Again, Regge theory describes interactions between hadrons at large values of rela-

tive energy and angular momenta. It enables one to describe the bulk of the production strength outside the resonance region. The latter is parameterized in terms of a few partial waves at low masses and spins. Parameters of the low-spin partial waves can be fitted to data and self-consistency between the low-energy (resonance) and high-energy (Regge) regions is checked/enforced through finite energy sum rules.

The leading Regge-pole dominance is an approximation, in principle valid at asymptotically large channel energies. At finite energies, the contribution from daughter trajectories and/or cuts may need to be examined on a case-by-case basis. The cut contribution typically accounts for diffraction in the final or initial state. To test the Regge exchange hypothesis one can also measure semi-inclusive production: beam + target $\rightarrow$ leading particle(s) + X, where "leading particles" have large-x [159]. This is described by some variant of Triple Regge coupling and so the "leading" part is beam + Reggeon $\rightarrow$ "leading particles" and so similar to case where X is a simple particle such as proton/neutron. Using arguments based on parton-hadron duality these can be further related the partonic structure functions [160].

4 Tools

[R.Mitchell]

One of the main challenges in experimental hadron spectroscopy is to determine whether or not a given data set contains evidence to support the existence of a previously unknown hadronic state (or states). The search for a new signal in experimental data consists of several steps: defining a theoretical model of the data; maximizing a likelihood function in order to fit the theoretical model to experimental data; and performing statistical tests to evaluate how well the model describes the data. The result of this process then allows one to *decide* whether or not a new state has been found, on the basis of model comparison.

While it is easy to list these steps, it has in the past not been straightforward to carry out this analysis procedure without incorporating approximations. The signals of interest are clearly not large ones (otherwise they would have already been identified!), and so we are at the stage of needing to move beyond crude approximate methods. The three steps of constructing a likelihood function based on a theoretical model, calculating the likelihood function with measured data, and evaluating the goodness-of-fit all require a set of tools that are both easy to use and contain state-of-the-art methods. Each step presents challenges:

1. How to incorporate theoretical innovations into data models (likelihood functions)?

2. How to perform efficient calculations of likelihood functions?

3. How to use statistical methods to evaluate how well theory describes data?

We now briefly summarize these issues, keeping in mind that the main framework will be a partial-wave analysis (PWA) of experimental data. In this, the key theoretical inputs are the *amplitudes* for participating processes. Afterwards, we list a few of the software tools that are currently being used and ideas for future collaborative code development.

4.1 Incorporation of theoretical innovations

The previous generation of amplitude analysis fitting tools had several undesirable features: they commonly assumed the "isobar model" with 2-body Breit–Wigner resonance decays; they were often easy to use, but were also a sort of black box, offering little flexibility to incorporate new amplitudes; and they were model-dependent, where the model-dependence had unquantifiable effects.

By contrast, the current generation of tools includes several desirable features: they allow more flexibility when defining amplitudes; they often

force the user to explicitly code the amplitudes, but are therefore less of a black box; they incorporate state of the art technology to increase fit speeds; and they allow systematic studies of model dependencies.

There are no longer *experimental* or *technological* barriers to incorporating theoretical innovations into experimental analyses. Several software packages exist that can perform fits to experimental data, using arbitrarily complicated amplitudes. An example of this is the `AmpTools` package[1] developed at Indiana University, described further below.

4.2 Efficient calculation of likelihood functions

For statistical accuracy, the number of events that need to be accumulated is $\mathcal{O}(10^6)$. In the search for a maximum of the likelihood function, therefore, each change in the parameters of the likelihood function will require $\mathcal{O}(10^6)$ evaluations of the likelihood function. What is fortunate is that there are ways to make use of the implicit parallelism in this calculation that utilize the latest developments in hardware technology. The overall trend is from multi-core to many-core processors, and from parallel to massively-parallel computing.

The most promising avenue for PWA is general purpose graphical processor unit (GPGPU) programming. Making use of the many cores on a GPU, likelihood calculations can be performed on many chunks of data at the same time. Presently there are several hardware-specific programming models (CUDA, OpenCL), but the field is in a state of rapid development. Another potential game changer is Intel's Many Integrated Core (MIC) architecture (Xeon Phi).

4.3 Statistical evaluation of results

Having obtained an unbinned maximum likelihood to obtain estimators for any unknown parameters, the question is then "How well does the probability density function (PDF) describe the data?" Unfortunately, an unbinned maximum likelihood does not provide any information that would help answer this question. Typically we (somehow) determine the "p-value." The p-value is the probability that a repeat of the experiment would have lesser agreement with the data than what we observe in our experiment.

In a binned analysis, this is often done by determining the χ^2 statistic. In many analyses, though, binning is not a viable option (due to high dimensions

[1] http://sourceforge.net/projects/amptools

and/or low statistics). There are many methods in the statistics literature that deal with these situations. However, one must take care to choose the right tool for the job, and ensure that one can properly validate any goodness-of-fit test [161].

4.4 Existing fitting tools and collaborative code development

A number of software packages currently exist to aid in amplitude analysis fits. Here we mention three: `AmpTools`, `ROOTPWA`, and `MadGraph`.

`AmpTools`, mentioned above, is a set of C++ classes that can be used for amplitude analyses. The key class is the Amplitude class, whose interface to the rest of the code is to take kinematics as input and output a complex number. The user supplies as many of these as needed. These amplitudes can be written either directly by theorists or by experimentalists in collaboration with theorists.

A new partial-wave analysis software package called `ROOTPWA`[2] has been developed at TU München. The goal of this project is to provide a common package for the analysis of multi-body final states produced in various reactions, such as diffractive dissociation, central production or muo-production. It includes a tool for the calculation of decay amplitudes, which is an improved implementation of the helicity-based isobar amplitude generator `gamp` from the `PWA2000` package originally developed at BNL, augmented by scripts for automatic symmetrization and testing. The amplitude calculator can be extended to different spin formalisms and is in principle not limited to isobar-like decay chains. The minimization is based on MINUIT2/MIGRAD which comes as part of the `ROOT` toolkit. `ROOTPWA` is completed by an n-body event generator and `ROOT`-based visualization tools.

For systematic amplitude generation, we can mention `MadGraph` [162]. `MadGraph`, developed at the University of Illinois and at Louvain University, is a helicity amplitude generator for tree-level Standard Model perturbation theory. It is open source and easily modifiable to include effective field theories[3]. Events can be generated with `MadEvent`, and cross sections and other observables can also be computed.

In order to make the best use of expertise to develop the best open-source software, the programming community has over the years evolved methods to make this collaboration work most efficiently. This practice is gradually being taken up in the physics research community as well. An outline of how

[2]The software is available under GPL at http://sourceforge.net/projects/rootpwa/.

[3]http://madgraph.phys.ucl.ac.be

a PWA community site might be structured is as follows:

- Common code repository (can link to already existing sourceforge repositories) containing:
  - Amplitude code
  - Data-readers
  - Minimizers
  - Integrators
  - Plotters
  - Parallelization libraries
  - Exchange ideas (code snippets)
  - Ecosystem of coexisting, independent codes

5 Concluding Remarks

The new generation of experiments in hadron physics that are flourishing around the world will in the foreseeable future continue to generate complex data sets, which demand a qualitatively new level of sophistication in analysis never before achieved. Amplitude analysis methods are urgently needed at hadron facilities to interpret the results experiments on non-perturbative quark/gluon interactions, however, it may turn out that physics beyond the Standard Model will also require tools developed to analyze strongly interacting systems. The aim of this document was to initiated the discussion on the methodology and tools needed to achieve these goals. We expect this discussion to continue through a series of workshops and schools that are planed for the near future. We hope these will lead to a development of state-of the-art analysis tools that will become available to practitioners in application and interpretation of amplitude analysis of the experimental data.

Bibliography

[1] J. Beringer et al. (Particle Data Group), Phys.Rev. **D86**, 010001 (2012).

[2] S. Durr, Z. Fodor, J. Frison, C. Hoelbling, R. Hoffmann, et al., Science **322**, 1224 (2008), 0906.3599.

[3] J. J. Dudek, R. G. Edwards, P. Guo, and C. E. Thomas, Phys. Rev. D 88, **094505** (2013), 1309.2608.

[4] J. J. Dudek, R. G. Edwards, M. J. Peardon, D. G. Richards, and C. E. Thomas, Phys.Rev. **D82**, 034508 (2010), 1004.4930.

[5] J. J. Dudek, R. G. Edwards, B. Joo, M. J. Peardon, D. G. Richards, et al., Phys.Rev. **D83**, 111502 (2011), 1102.4299.

[6] L. Liu et al. (Hadron Spectrum Collaboration), JHEP **1207**, 126 (2012), 1204.5425.

[7] R. G. Edwards, J. J. Dudek, D. G. Richards, and S. J. Wallace, Phys.Rev. **D84**, 074508 (2011), 1104.5152.

[8] R. G. Edwards, N. Mathur, D. G. Richards, and S. J. Wallace, Phys.Rev. **D87**, 054506 (2013), 1212.5236.

[9] J. J. Dudek and R. G. Edwards, Phys.Rev. **D85**, 054016 (2012), 1201.2349.

[10] C. J. Morningstar and M. J. Peardon, Phys.Rev. **D60**, 034509 (1999), hep-lat/9901004.

[11] Y. Chen, A. Alexandru, S. Dong, T. Draper, I. Horvath, et al., Phys.Rev. **D73**, 014516 (2006), hep-lat/0510074.

[12] M. Luscher, Nucl.Phys. **B354**, 531 (1991).

[13] K. Rummukainen and S. A. Gottlieb, Nucl.Phys. **B450**, 397 (1995), hep-lat/9503028.

[14] C. Kim, C. Sachrajda, and S. R. Sharpe, Nucl.Phys. **B727**, 218 (2005), hep-lat/0507006.

[15] N. H. Christ, C. Kim, and T. Yamazaki, Phys.Rev. **D72**, 114506 (2005), hep-lat/0507009.

[16] R. A. Briceno and Z. Davoudi, Phys. Rev. D. 88, **094507**, 094507 (2013), 1204.1110.

[17] M. T. Hansen and S. R. Sharpe, Phys.Rev. **D86**, 016007 (2012), 1204.0826.

[18] P. Guo, J. Dudek, R. Edwards, and A. P. Szczepaniak, Phys.Rev. **D88**, 014501 (2013), 1211.0929.

[19] J. J. Dudek, R. G. Edwards, and C. E. Thomas, Phys.Rev. **D87**, 034505 (2013), 1212.0830.

[20] R. A. Briceno and Z. Davoudi, Phys.Rev. **D87**, 094507 (2013), 1212.3398.

[21] M. T. Hansen and S. R. Sharpe (2013), 1311.4848.

[22] G. Chew, M. Goldberger, F. Low, and Y. Nambu, Phys.Rev. **106**, 1345 (1957).

[23] A. Sibirtsev, J. Haidenbauer, F. Huang, S. Krewald, and U.-G. Meißner, Eur.Phys.J. **A40**, 65 (2009), 0903.0535.

[24] A. Sibirtsev, J. Haidenbauer, S. Krewald, U.-G. Meißner, and A. Thomas, Eur.Phys.J. **A41**, 71 (2009), 0902.1819.

[25] A. Sibirtsev, J. Haidenbauer, S. Krewald, T. Lee, U.-G. Meißner, et al., Eur.Phys.J. **A34**, 49 (2007), 0706.0183.

[26] J. Laget, Phys.Lett. **B695**, 199 (2011), 1004.1949.

[27] J. Laget, Phys.Lett. **B685**, 146 (2010), 0912.1942.

[28] B. G. Yu, T. K. Choi, and W. Kim, Phys.Rev. **C83**, 025208 (2011), 1103.1203.

[29] M. Guidal, J. Laget, and M. Vanderhaeghen, Phys.Rev. **C68**, 058201 (2003), hep-ph/0308131.

[30] W.-T. Chiang, S. N. Yang, L. Tiator, M. Vanderhaeghen, and D. Drechsel, Phys.Rev. **C68**, 045202 (2003), nucl-th/0212106.

[31] A. Sibirtsev, J. Haidenbauer, S. Krewald, and U.-G. Meißner, Eur.Phys.J. **A46**, 359 (2010), 1007.3140.

[32] F. Huang, A. Sibirtsev, J. Haidenbauer, S. Krewald, and U.-G. Meißner, Eur.Phys.J. **A44**, 81 (2010), 0910.4275.

[33] F. Huang, A. Sibirtsev, S. Krewald, C. Hanhart, J. Haidenbauer, et al., Eur.Phys.J. **A40**, 77 (2009), 0810.2680.

[34] R. Arndt, W. Briscoe, I. Strakovsky, R. Workman, and M. Pavan, Phys.Rev. **C69**, 035213 (2004), nucl-th/0311089.

[35] W.-T. Chiang, S.-N. Yang, L. Tiator, and D. Drechsel, Nucl.Phys. **A700**, 429 (2002), nucl-th/0110034.

[36] G. Penner and U. Mosel, Phys.Rev. **C66**, 055212 (2002), nucl-th/0207069.

[37] M. Battaglieri et al. (CLAS Collaboration), Phys.Rev. **D80**, 072005 (2009), 0907.1021.

[38] V. Dorofeev et al. (VES Collaboration), AIP Conf.Proc. **619**, 143 (2002), hep-ex/0110075.

[39] T. Schluter, D. Ryabchikov, W. Dunnweber, and M. Faessler (COMPASS Collaboration), PoS **QNP2012**, 074 (2012), 1207.1076.

[40] J. Gerard and J. Weyers, Eur.Phys.J. **C7**, 1 (1999), hep-ph/9711469.

[41] J. Gerard, J. Pestieau, and J. Weyers, Phys.Lett. **B436**, 363 (1998), hep-ph/9803328.

[42] R. Akhmetshin et al. (CMD2 Collaboration), Phys.Lett. **B466**, 392 (1999), hep-ex/9904024.

[43] R. Akhmetshin et al. (CMD-2 Collaboration), Phys.Lett. **B595**, 101 (2004), hep-ex/0404019.

[44] R. A. Briere et al. (CLEO Collaboration), Phys.Rev. **D62**, 072003 (2000), hep-ex/0004028.

[45] B. Aubert et al. (BaBar Collaboration), Phys.Rev. **D71**, 052001 (2005), hep-ex/0502025.

[46] J. Lees et al. (BaBar Collaboration), Phys.Rev. **D85**, 112009 (2012), 1201.5677.

[47] V. Aulchenko et al. (KEDR Collaboration), Phys.Lett. **B573**, 63 (2003), hep-ex/0306050.

[48] V. Anashin et al. (KEDR Collaboration), Phys.Lett. **B685**, 134 (2010), 0912.1082.

[49] V. Anashin, V. Aulchenko, E. Baldin, A. Barladyan, A. Y. Barnyakov, et al., Phys.Lett. **B711**, 280 (2012), 1109.4215.

[50] V. Anashin, V. Aulchenko, E. Baldin, A. Barladyan, A. Y. Barnyakov, et al., Phys.Lett. **B711**, 292 (2012), 1109.4205.

[51] V. Anashin et al. (KEDR Collaboration), Phys.Lett. **B686**, 84 (2010), 0909.5545.

[52] S. Eidelman et al. (KEDR Collaboration), Nucl.Phys.Proc.Suppl. **218**, 155 (2011).

[53] V. Anashin et al. (KEDR Collaboration), Phys.Lett. **B703**, 543 (2011), 1107.2824.

[54] D. Asner, T. Barnes, J. Bian, I. Bigi, N. Brambilla, et al., Int.J.Mod.Phys. **A24**, S1 (2009), 0809.1869.

[55] J. Alves, A. Augusto et al. (LHCb Collaboration), JINST **3**, S08005 (2008).

[56] R. Aaij et al. (LHCb Collaboration), Phys.Lett. **B694**, 209 (2010), 1009.2731.

[57] R. Aaij et al. (LHCb collaboration), Nucl.Phys. **B871**, 1 (2013), 1302.2864.

[58] J. Charles, O. Deschamps, S. Descotes-Genon, R. Itoh, H. Lacker, et al., Phys.Rev. **D84**, 033005 (2011), 1106.4041.

[59] R. Aaij et al. (LHCb Collaboration), Phys.Rev. **D85**, 091105 (2012), 1203.3592.

[60] R. Aaij et al. (LHCb collaboration), Phys.Rev. **D87**, 112010 (2013), 1304.2600.

[61] R. Aaij et al. (LHCb Collaboration), Phys.Rev. **D84**, 112008 (2011), 1110.3970.

[62] R. Aaij et al. (LHCb collaboration), JHEP **1306**, 112 (2013), 1303.4906.

[63] L. collaboration (LHCb collaboration) (2012).

[64] R. Aaij et al. (LHCb collaboration), Phys.Rev.Lett. **111**, 101801 (2013), 1306.1246.

[65] R. Aaij et al. (LHCb Collaboration), Phys.Lett. **B718**, 43 (2012), 1209.5869.

[66] R. Aaij et al. (LHCb collaboration), Phys.Rev. **D87**, 072004 (2013), 1302.1213.

[67] R. Aaij et al. (LHCb collaboration) (2013), 1307.7648.

[68] R. Aaij et al. (LHCb collaboration), Phys.Rev. **D88**, 052002 (2013), 1307.2782.

[69] A. Giri, Y. Grossman, A. Soffer, and J. Zupan, Phys.Rev. **D68**, 054018 (2003), hep-ph/0303187.

[70] D. Atwood and A. Soni, Phys.Rev. **D68**, 033003 (2003), hep-ph/0304085.

[71] A. Bondar and A. Poluektov (2007), hep-ph/0703267.

[72] A. Bondar, A. Poluektov, and V. Vorobiev, Phys.Rev. **D82**, 034033 (2010), 1004.2350.

[73] N. Lowrey et al. (CLEO Collaboration), Phys.Rev. **D80**, 031105 (2009), 0903.4853.

[74] J. Libby et al. (CLEO Collaboration), Phys.Rev. **D82**, 112006 (2010), 1010.2817.

[75] R. A. Briere et al. (CLEO Collaboration), Phys.Rev. **D80**, 032002 (2009), 0903.1681.

[76] R. Aaij et al. (LHCb collaboration) (2013), 1305.2050.

[77] R. Aaij et al. (LHCb collaboration), Phys.Lett. **B723**, 44 (2013), 1303.4646.

[78] J. Rademacker and G. Wilkinson, Phys.Lett. **B647**, 400 (2007), hep-ph/0611272.

[79] 1241820 (2013), 1307.2022.

[80] A. Martin and T. Spearman, Elementary Particle Theory (North Holland Publishing Co. Amsterdam, 1970).

[81] M. Perl., High Energy Hadron Physics (John Wiley and Sons. New York, 1975).

[82] M. L. Goldberger and K. M. Watson, Collision Theory (John Wiley and Sons. New York, 1965).

[83] J. Gasser and G. Wanders, Eur.Phys.J. **C10**, 159 (1999), hep-ph/9903443.

[84] G. Wanders, Eur.Phys.J. **C17**, 323 (2000), hep-ph/0005042.

[85] B. Ananthanarayan, G. Colangelo, J. Gasser, and H. Leutwyler, Phys.Rept. **353**, 207 (2001), hep-ph/0005297.

[86] P. Büttiker, S. Descotes-Genon, and B. Moussallam, Eur.Phys.J. **C33**, 409 (2004), hep-ph/0310283.

[87] I. Caprini, G. Colangelo, and H. Leutwyler, Phys.Rev.Lett. **96**, 132001 (2006), hep-ph/0512364.

[88] R. García-Martín, R. Kamiński, J. Peláez, and J. Ruiz de Elvira, Phys.Rev.Lett. **107**, 072001 (2011), 1107.1635.

[89] S. Descotes-Genon and B. Moussallam, Eur.Phys.J. **C48**, 553 (2006), hep-ph/0607133.

[90] P. Hoyer and J. Kwiecinski, Nucl. Phys. **B60**, 26 (1973).

[91] S. Roy, Phys.Lett. **B36**, 353 (1971).

[92] F. Steiner, Fortsch.Phys. **19**, 115 (1971).

[93] G. Hite and F. Steiner, Nuovo Cim. **A18**, 237 (1973).

[94] G. Colangelo, J. Gasser, and H. Leutwyler, Nucl.Phys. **B603**, 125 (2001), hep-ph/0103088.

[95] R. Kamiński, L. Lesniak, and B. Loiseau, Phys.Lett. **B551**, 241 (2003), hep-ph/0210334.

[96] J. Peláez and F. Ynduráin, Phys.Rev. **D71**, 074016 (2005), hep-ph/0411334.

[97] R. García-Martín, R. Kamiński, J. Peláez, J. Ruiz de Elvira, and F. Ynduráin, Phys.Rev. **D83**, 074004 (2011), 1102.2183.

[98] J. A. Oller, L. Roca, and C. Schat, Phys.Lett. **B659**, 201 (2008), 0708.1659.

[99] M. Hoferichter, D. R. Phillips, and C. Schat, Eur.Phys.J. **C71**, 1743 (2011), 1106.4147.

[100] R. García-Martín and B. Moussallam, Eur.Phys.J. **C70**, 155 (2010), 1006.5373.

[101] B. Moussallam, Eur.Phys.J. **C71**, 1814 (2011), 1110.6074.

[102] C. Ditsche, M. Hoferichter, B. Kubis, and U.-G. Meißner, JHEP **1206**, 043 (2012), 1203.4758.

[103] M. Froissart, Phys.Rev. **123**, 1053 (1961).

[104] A. Martin, Phys.Rev. **129**, 1432 (1963).

[105] J. Peláez and F. Ynduráin, Phys.Rev. **D69**, 114001 (2004), hep-ph/0312187.

[106] F. Halzen, K. Igi, M. Ishida, and C. Kim, Phys.Rev. **D85**, 074020 (2012), 1110.1479.

[107] I. Caprini, G. Colangelo, and H. Leutwyler, Eur.Phys.J. **C72**, 1860 (2012), 1111.7160.

[108] K. M. Watson, Phys.Rev. **95**, 228 (1954).

[109] E. Fermi, Nuovo Cim. **2S1**, 17 (1955).

[110] R. Omnes, Nuovo Cim. **8**, 316 (1958).

[111] N. I. Muskhelishvili, Singular Integral Equations (Wolters-Noordhoff Publishing, Groningen, 1953).

[112] M. Gorchtein, P. Guo, and A. P. Szczepaniak, Phys.Rev. **C86**, 015205 (2012), 1102.5558.

[113] C. Hanhart, Phys.Lett. **B715**, 170 (2012), 1203.6839.

[114] B. Ananthanarayan, I. Caprini, and I. Sentitemsu Imsong, Eur.Phys.J. **A47**, 147 (2011), 1108.0284.

[115] G. Abbas, B. Ananthanarayan, I. Caprini, I. Sentitemsu Imsong, and S. Ramanan, Eur.Phys.J. **A44**, 175 (2010), 0912.2831.

[116] A. P. Szczepaniak, P. Guo, M. Battaglieri, and R. De Vita, Phys.Rev. **D82**, 036006 (2010), 1005.5562.

[117] G. Abbas, B. Ananthanarayan, I. Caprini, and I. Sentitemsu Imsong, Phys.Rev. **D82**, 094018 (2010), 1008.0925.

[118] P. Guo, R. Mitchell, and A. P. Szczepaniak, Phys.Rev. **D82**, 094002 (2010), 1006.4371.

[119] N. Khuri and S. Treiman, Phys.Rev. **119**, 1115 (1960).

[120] F. Stollenwerk, C. Hanhart, A. Kupsc, U.-G. Meißner, and A. Wirzba, Phys.Lett. **B707**, 184 (2012), 1108.2419.

[121] M. Hoferichter, B. Kubis, and D. Sakkas, Phys.Rev. **D86**, 116009 (2012), 1210.6793.

[122] J. Kambor, C. Wiesendanger, and D. Wyler, Nucl.Phys. **B465**, 215 (1996), hep-ph/9509374.

[123] G. Colangelo, S. Lanz, and E. Passemar, PoS **CD09**, 047 (2009), 0910.0765.

[124] S. P. Schneider, B. Kubis, and C. Ditsche, JHEP **1102**, 028 (2011), 1010.3946.

[125] F. Niecknig, B. Kubis, and S. P. Schneider, Eur.Phys.J. **C72**, 2014 (2012), 1203.2501.

[126] J. F. Donoghue, J. Gasser, and H. Leutwyler, Nucl.Phys. **B343**, 341 (1990).

[127] B. Moussallam, Eur.Phys.J. **C14**, 111 (2000), hep-ph/9909292.

[128] S. Descotes-Genon, JHEP **0103**, 002 (2001), hep-ph/0012221.

[129] M. Hoferichter, C. Ditsche, B. Kubis, and U.-G. Meißner, JHEP **1206**, 063 (2012), 1204.6251.

[130] J. Daub, H. Dreiner, C. Hanhart, B. Kubis, and U.-G. Meißner, JHEP **1301**, 179 (2013), 1212.4408.

[131] M. Jamin, J. A. Oller, and A. Pich, Nucl.Phys. **B622**, 279 (2002), hep-ph/0110193.

[132] M. Döring, U.-G. Meißner, and W. Wang, JHEP **1310**, 011 (2013), 1307.0947.

[133] S. Ceci, M. Döring, C. Hanhart, S. Krewald, U.-G. Meißner, et al., Phys.Rev. **C84**, 015205 (2011), 1104.3490.

[134] H. Kamano, S. Nakamura, T. S. H. Lee, and T. Sato, Phys.Rev. **C88**, 035209 (2013), 1305.4351.

[135] D. Rönchen, M. Döring, F. Huang, H. Haberzettl, J. Haidenbauer, C. Hanhart, S. Krewald, U.-G. Meiß, and K. Nakayama (2014), 1401.0634.

[136] D. Rönchen, M. Döring, F. Huang, H. Haberzettl, J. Haidenbauer, C. Hanhart, S. Krewald, U.-G. Meißß, and K. Nakayama, Eur.Phys.J. **A49**, 44 (2013), 1211.6998.

[137] L. Tiator, S. Kamalov, S. Ceci, G. Chen, D. Drechsel, et al., Phys.Rev. **C82**, 055203 (2010), 1007.2126.

[138] C. Schütz, J. Durso, K. Holinde, and J. Speth, Phys.Rev. **C49**, 2671 (1994).

[139] R. Aaron, R. Amado, and J. Young, Phys.Rev. **174**, 2022 (1968).

[140] H. Kamano, S. Nakamura, T. Lee, and T. Sato, Phys.Rev. **D84**, 114019 (2011), 1106.4523.

[141] P. Magalhaes, M. Robilotta, K. Guimaraes, T. Frederico, W. de Paula, et al., Phys.Rev. **D84**, 094001 (2011), 1105.5120.

[142] R. L. Workman, M. W. Paris, W. J. Briscoe, and I. I. Strakovsky, Phys.Rev. **C86**, 015202 (2012), 1202.0845.

[143] A. Anisovich, R. Beck, E. Klempt, V. Nikonov, A. Sarantsev, and U. Thoma, Eur. Phys. J. **A48**, 15 (2012).

[144] A. V. Anisovich, R. Beck, E. Klempt, V. Nikonov, A. V. Sarantsev, and U. Thoma, Eur. Phys. J. **A48**, 88 (2012).

[145] V. Shklyar, H. Lenske, U. Mosel, and G. Penner, Phys. Rev. **C71**, 055206 (2005).

[146] V. Shklyar, H. Lenske, and U. Mosel, Phys.Rev. **C87**, 015201 (2013), 1206.5414.

[147] D. Drechsel, S. Kamalov, and L. Tiator, Eur.Phys.J. **A34**, 69 (2007), 0710.0306.

[148] H. Zhang, J. Tulpan, M. Shrestha, and D. Manley, Phys.Rev. **C88**, 035205 (2013), 1305.4575.

[149] M. Batinic, S. Ceci, A. Svarc, and B. Zauner, Phys.Rev. **C82**, 038203 (2010).

[150] R. L. Workman and R. A. Arndt, Phys.Rev. **D45**, 1789 (1992).

[151] A. Anisovich, E. Klempt, V. Nikonov, A. Sarantsev, and U. Thoma, Eur.Phys.J. **A49**, 158 (2013), 1310.3610.

[152] P. Collins, Phys.Rept. **1**, 103 (1971).

[153] P. Collins (1977).

[154] R. Dolen, D. Horn, and C. Schmid, Phys.Rev.Lett. **19**, 402 (1967).

[155] R. Dolen, D. Horn, and C. Schmid, Phys.Rev. **166**, 1768 (1968).

[156] J. Mandula, J. Weyers, and G. Zweig, Ann.Rev.Nucl.Part.Sci. **20**, 289 (1970).

[157] R. Phillips and D. Roy, Rept.Prog.Phys. **37**, 1035 (1974).

[158] G. Fox (CMD2 Collaboration) (2003).

[159] A. Barnes, G. Fox, R. Kennett, R. Walker, O. Dahl, et al., Nucl.Phys. **B145**, 45 (1978).

[160] J. Bjorken and J. B. Kogut, Phys.Rev. **D8**, 1341 (1973).

[161] M. Williams, JINST **5**, P09004 (2010), 1006.3019.

[162] J. Alwall, M. Herquet, F. Maltoni, O. Mattelaer, and T. Stelzer, JHEP **1106**, 128 (2011), 1106.0522.